

Pseudospin anisotropy classification of quantum Hall ferromagnets

T. Jungwirth^{1,2} and A. H. MacDonald¹

¹*Department of Physics, Indiana University, Bloomington, Indiana 47405*

²*Institute of Physics ASCR, Cukrovarnická 10, 162 00 Praha 6, Czech Republic*

(Received 27 March 2000; published 22 December 2000)

Broken-symmetry ground states with uniform electron density are common in quantum Hall systems when two Landau levels simultaneously approach the chemical potential at integer filling factor ν . The close analogy between these two-dimensional electron system states and conventional itinerant electron ferromagnets can be emphasized by using a pseudospin label to distinguish the two Landau levels. As in conventional ferromagnets, the evolution of the system's state as external field parameters are varied is expected to be sensitive to the dependence of ground-state energy on pseudospin orientation. We discuss the predictions of Hartree-Fock theory for the dependence of the sign and magnitude of the pseudospin anisotropy energy on the nature of the crossing Landau levels. We build up a classification scheme for quantum Hall ferromagnets that applies for single layer and bilayer systems with two aligned Landau levels distinguished by any combination of real spin, orbit radius, or growth direction degree-of-freedom quantum numbers. The possibility of *in situ* tuning between easy-axis and easy-plane quantum Hall ferromagnets is discussed for biased bilayer systems with total filling factors $\nu=3$ or $\nu=4$. Detailed predictions are made for the bias dependence of pseudospin reversal properties in $\nu=3$ bilayer systems.

DOI: 10.1103/PhysRevB.63.035305

PACS number(s): 73.43.-f, 75.10.Lp, 75.30.Gw

I. INTRODUCTION

Studies of magnetic phenomena in semiconductors have opened fruitful new ways to explore the subtleties of quantum magnetism. In quantum Hall samples, the tunability of semiconductor electronic systems and the quantization of single-particle energies into macroscopically degenerate Landau levels (LLs) combine to open up a rich and varied phenomenology. The effective zero width of electronic energy bands enhances the role of inter-particle interactions¹ and can frequently lead to the formation of ordered many-particle ground states, including ferromagnetic ones.

Most studies of quantum Hall ferromagnets² (QHF) have focused on spontaneous spin-alignment in a single-layer two-dimensional (2D) electron system at LL filling factor $\nu=1$. In this case, it turns out that electron-electron interactions favor fully aligned electron spins even in the limit of vanishingly small Zeeman coupling^{2,3} and the ferromagnetic ground state of the system is described exactly by Hartree-Fock (HF) theory. Because of the near spin independence of the Coulomb interaction, the $\nu=1$ single-layer QHF is a Heisenberg-like isotropic two-dimensional ferromagnet. One of the unique properties of this simple itinerant electron ferromagnet is that its instantons³ (skyrmions) carry charge and can be observed⁴ in the ground states at filling factors slightly deviating from 1.

The notion of the QHF can be generalized, however. It turns out that, at least according to HF theory, broken-symmetry ground states occur at integer filling factors in quantum Hall systems any time two or more valence LLs are degenerate and the number of electrons is sufficient to fill only some of the LLs. In effect, electrons in the ordered state occupy spontaneously generated LLs that are linear combinations of the single-particle levels chosen to minimize the electron interaction energy.

The simplest example of a pseudospin QHF obtains at ν

$=1$ in balanced bilayer 2D systems where the single-particle LLs in the two layers are degenerate. In the ordered ground state,^{2,5,6} the electrons occupy a LL that is a linear combination of the isolated layer levels, forming a state with spontaneous interlayer phase coherence. Recently, Josephson-like behavior seen⁷ in 2D-to-2D tunneling spectroscopy studies of bilayer systems has provided a direct manifestation of collective behavior generated by this broken symmetry. In $\nu=1$ bilayer systems, the broken-symmetry state minimizes the Hartree energy cost by distributing charge equally between layers and gives up part of the intralayer exchange energy while gaining more in interlayer exchange energy. Unlike the single layer $\nu=1$ QHF, the ordered HF ground state is not exact in this case, and the order predicted by HF theory can be destroyed. With decreasing interlayer exchange energy, quantum fluctuations around the mean-field ordered state become more important, and for layer separations larger than approximately two magnetic lengths, fluctuations destroy the spontaneous coherence. The corresponding order-disorder quantum phase transition has been observed experimentally.⁸ In $\nu=1$ bilayer QHFs, it is the layer degree of freedom that is represented as a *pseudospin*- $\frac{1}{2}$. With this mapping the phase-coherent state is equivalent to a spin- $\frac{1}{2}$ easy-plane ferromagnet. Finite-temperature Kosterlitz-Thouless phase transition,⁹ continuous quantum phase transition induced by an in-plane magnetic field,⁸ and macroscopic collective transport effects⁷ are among the remarkable phenomena which have been studied on bilayer QHFs.

Recent experiments in single-layer¹⁰ and bilayer¹¹ 2D systems at even-integer filling factors have further enlarged the field of quantum Hall ferromagnetism. It has been shown that easy-axis ferromagnetic ground states can occur¹⁰ at higher filling factors when LLs with different orbit radius quantum numbers are brought close to alignment.^{12,10} In HF language, easy-axis anisotropy means that many-body states

with either of the two aligned LLs completely filled and the other empty are energetically more favorable than the coherent superposition state. The easy-axis pseudospin anisotropy occurs in this case because intra-LL exchange is stronger than exchange between particles from LLs with different orbit radius quantum numbers. Transport measurements^{11,13} have demonstrated that easy-axis QHFs exhibit hysteresis with a complicated phenomenology, presumably associated with an interplay between disorder and domain morphology similar to that in conventional thin-film magnets.

In this paper, we classify QHFs according to their pseudospin anisotropy energies as either isotropic, easy-axis, or easy-plane systems. We report on a HF-based analysis that predicts how the class of broken-symmetry ground states depends on the nature of the crossing LLs. In some cases, competing effects allow the anisotropy energy to be tuned continuously generating a zero-temperature quantum phase transition between different classes of states. We consider only cases in which no more than two LLs are nearly degenerate and the number of electrons is sufficient to occupy one of them. We will always assume that lower-energy LLs, if present, are completely full and higher-energy LLs are completely empty; coupling to these remote LLs can usually be treated perturbatively if necessary, although we do not do so explicitly here. An important example of an instance in which more than two LLs are close to degeneracy pertains in double-layer systems with weak tunneling and weak Zeeman coupling;^{14,15} we do not treat this or other more complex cases with many degenerate LLs in this paper. In Sec. II, we precisely define the pseudospin language we use in which one of the LLs is referred to as the pseudospin-up state and the other LL as the pseudospin-down state. Since we assume that the magnetic field is perpendicular to the 2D electron layer, growth direction and in-plane degrees of freedom decouple. The pseudospin quantum number then subsumes real spin, orbit radius, and growth direction (subband) degrees of freedom. To make the discussion more transparent, we concentrate on a system consisting of two nearby infinitely narrow 2D layers, the simplest model that has a nontrivial growth direction degree of freedom. Comments are made throughout the text about realistic samples with more complicated geometries. In Sec. III, we derive a general expression for the HF ground-state energy in the pseudospin ferromagnetic state. Section IV summarizes the rather cumbersome evaluation of Coulomb interaction matrix elements. Readers not interested in technical details of the calculation are encouraged to skip to Sec. V, where we present our conclusions concerning pseudospin magnetic anisotropy of single layer and bilayer QHFs. This section includes phase diagrams that show the regimes of physically tunable parameters with easy-axis and easy-plane anisotropies. Symmetry-breaking fields and the dynamics of pseudospin reversal are discussed in Sec. VI. Finally, we conclude in Sec. VII with a brief summary of the main results of our paper.

II. PSEUDOSPIN REPRESENTATION

The pseudospin language was introduced⁵ to the description of broken-symmetry states in the quantum Hall regime

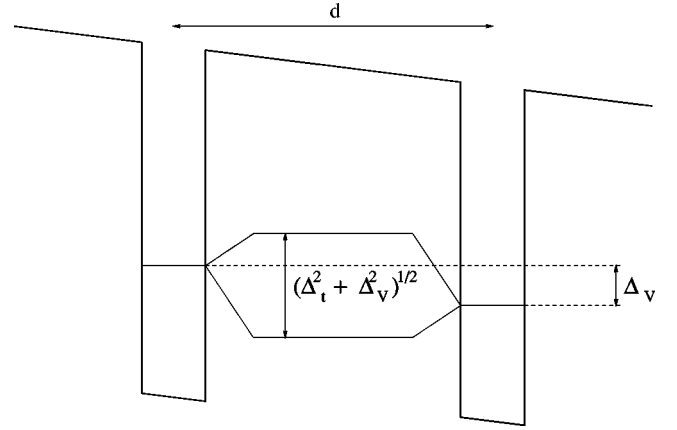


FIG. 1. Schematic of the conduction-band edge profile of a biased double-quantum-well sample with nonzero tunneling between 2D layers. Energy levels due to quantization of electron motion along the growth direction are also indicated. For concrete calculations, we assume infinitely narrow quantum wells separated by the distance d .

in order to draw on the analogy between double-quantum-well systems at $\nu=1$ and 2D ferromagnets. In that work, the pseudospin degree of freedom represented the layer index of a bilayer system. Here we allow the pseudospin index to have a more general meaning. To establish terminology, it is useful to recall the single-particle spectrum of a bilayer 2D system subject to a perpendicular magnetic field. Quantum-well subbands of individual layers can be mixed by inter-layer tunneling and shifted by the application of a bias potential. We limit our attention to the usual case in which only the lowest electric subband of either quantum well is occupied, and for explicit calculations we use a zero-width quantum-well model. Allowing for external bias and for tunneling between the wells (see Fig. 1), the bilayer subband wave functions of the zero-width model are

$$\lambda_{\pm 1}(z) = \frac{1}{\sqrt{2}} [\sqrt{(1 \mp r_{\Delta}) \delta(z)} \pm \sqrt{(1 \pm r_{\Delta}) \delta(z-d)}], \quad (1)$$

where $\delta(z)$ is the Dirac's delta function, $r_{\Delta} = \Delta_V / (\Delta_V^2 + \Delta_t^2)^{1/2}$, Δ_V is the bias potential, Δ_t the tunneling gap at zero bias, and d is the layer separation. To account for specific experimental samples, finite width effects can be incorporated by replacing the wave functions (1) with electric subband wave functions calculated using the self-consistent local-spin-density-approximation (LSDA) model.¹⁶

In the Landau gauge, the wave functions in the 2D plane take a form $\phi_{n,s,k}(x) \exp(iky) / \sqrt{L_y}$, where

$$\phi_{n,s,k}(x) = [\pi l^2 2^{2n} (n!)^2]^{-1/4} H_n \left(\frac{x - l^2 k}{l} \right) \times \exp \left[-\frac{(x - l^2 k)^2}{2l^2} \right], \quad (2)$$

k is the wave-vector label that distinguishes states within a LL, $n=0,1,\dots$ is the orbit radius quantum number, l is the

magnetic length, and we have also explicitly included the real spin, $s = \pm \frac{1}{2}$, degree of freedom. The single-particle energy spectrum consists of discrete LLs,

$$E_{\xi,n,s} = -\frac{\xi}{2}(\Delta_V^2 + \Delta_I^2)^{1/2} + \hbar\omega_c(n + \frac{1}{2}) - s|g|\mu_B B, \quad (3)$$

where $\xi = \pm 1$ is the subband index, ω_c is the cyclotron frequency, and the last term is the real-spin Zeeman coupling. Each LL has a macroscopic degeneracy with the number of orbital states per level $N_\phi = AB/\Phi_0$, where A is the system area, B is the field strength, and Φ_0 is the magnetic flux quantum.

The many-body broken-symmetry states we study in the following sections occur when two LLs are brought close to alignment while remaining sufficiently separated from other LLs. In our calculations, each LL can have one of two possible subband indices, one of two possible spin indices, and any value for the 2D cyclotron orbit kinetic-energy index. The two crossing LLs can differ in any or all of these labels. We label one of the two levels as the pseudospin-up ($\sigma = \uparrow$) state and the other level as the pseudospin-down ($\sigma = \downarrow$) state. We truncate the single-particle Hilbert space by ignoring higher LLs and introducing effective one-body fields that account for the effect of electrons in lower LLs on the two pseudospin states. Within this model, the set of single-particle states reduces to the following wave functions:

$$\psi_{\sigma,k}(\vec{r}) = \lambda_{\xi(\sigma)}(z) \phi_{n(\sigma),s(\sigma),k}(x) \frac{\exp(iky)}{\sqrt{L_y}}. \quad (4)$$

A particle with the pseudospin oriented along a general unit vector $\hat{m} = (\sin\theta\cos\varphi, \sin\theta\sin\varphi, \cos\theta)$ is described by

$$\psi_{\hat{m},k}(\vec{r}) = \cos\left(\frac{\theta}{2}\right) \psi_{\uparrow,k}(\vec{r}) + \sin\left(\frac{\theta}{2}\right) e^{i\varphi} \psi_{\downarrow,k}(\vec{r}). \quad (5)$$

III. MANY-BODY HAMILTONIAN AND HF TOTAL ENERGY

In the HF approximation, the QHF has a single Slater determinant state with the same pseudospin orientation for every orbital k . In this section, we derive general expressions for the dependence of the many-electron state energy on pseudospin orientation. It is convenient to express the many-body Hamiltonian using Pauli spin matrices τ_x , τ_y , and τ_z and the 2×2 identity matrix, which we label τ_1 . In this representation, the Hamiltonian reads

$$\begin{aligned} H = & - \sum_{i=1,x,y,z} \sum_{k=1}^{N_\phi} \sum_{\alpha,\alpha'=1}^2 b_i \tau_i^{\alpha',\alpha} c_{\sigma(\alpha'),k}^\dagger c_{\sigma(\alpha),k} \\ & + \frac{1}{2} \sum_{i,j=1,x,y,z} \sum_{k_1,k'_1}^{N_\phi} \sum_{\alpha_1,\alpha'_1}^2 \sum_{k_2,k'_2=1}^2 W_{i,j}^{k'_1,k'_2,k_1,k_2} \tau_i^{\alpha'_1,\alpha_1} \tau_j^{\alpha'_2,\alpha_2} \\ & \times c_{\sigma(\alpha'_1),k'_1}^\dagger c_{\sigma(\alpha'_2),k'_2}^\dagger c_{\sigma(\alpha_2),k_2} c_{\sigma(\alpha_1),k_1}, \end{aligned} \quad (6)$$

TABLE I. Coulomb interaction matrix elements $W_{i,j}$; $i,j = 1,x,y,z$. The B_n^\pm terms are defined in Eqs. (8).

	1	x	y	z
1	$B_1^+ + B_2^+$	$B_5^- + B_6^+$	$\frac{1}{i}B_5^- + \frac{1}{i}B_6^-$	$B_1^- - B_2^-$
x	$B_7^+ + B_8^+$	$B_3^+ + B_4^+$	$\frac{1}{i}B_3^- - \frac{1}{i}B_4^-$	$B_7^- - B_8^-$
y	$\frac{1}{i}B_7^- + \frac{1}{i}B_8^-$	$\frac{1}{i}B_3^- + \frac{1}{i}B_4^-$	$B_3^+ - B_4^+$	$\frac{1}{i}B_7^- - \frac{1}{i}B_8^-$
z	$B_1^- + B_2^-$	$B_5^+ - B_6^+$	$\frac{1}{i}B_5^- - \frac{1}{i}B_6^-$	$B_1^+ - B_2^+$

where $\sigma(1) = \uparrow$ and $\sigma(2) = \downarrow$. The one-body terms b_i include, in general, the external bias potential, tunneling, cyclotron, and Zeeman energies, and also the mean field from interactions with electrons in the frozen LLs lying below the $\sigma = \uparrow$ and \downarrow levels. We will give an explicit expression for b_i in Sec. VI. Here and in the following two sections, we concentrate on the two-body terms in the Hamiltonian (6).

The potentials $W_{i,j}$ represent different combinations of Coulomb interaction matrix elements, $V_{\sigma'_1,\sigma'_2,\sigma_1,\sigma_2}$, of the single-particle pseudospin states,

$$\begin{aligned} V_{\sigma'_1,\sigma'_2,\sigma_1,\sigma_2}^{k'_1,k'_2,k_1,k_2} = & \int d^3\vec{r}_1 \int d^3\vec{r}_2 \psi_{\sigma'_1,k'_1}^*(\vec{r}_1) \psi_{\sigma'_2,k'_2}^*(\vec{r}_2) \\ & \times \frac{e^2}{\epsilon|\vec{r}_1 - \vec{r}_2|} \psi_{\sigma_1,k_1}(\vec{r}_1) \psi_{\sigma_2,k_2}(\vec{r}_2). \end{aligned} \quad (7)$$

General expressions for the pseudospin-dependent interactions $W_{i,j}$ are given in Table I in terms of the following matrix element combinations:

$$\begin{aligned} B_1^\pm &= \frac{1}{4}(V_{\uparrow,\uparrow,\uparrow,\uparrow} \pm V_{\downarrow,\downarrow,\downarrow,\downarrow}), & B_2^\pm &= \frac{1}{4}(V_{\uparrow,\downarrow,\downarrow,\downarrow} \pm V_{\downarrow,\uparrow,\uparrow,\uparrow}), \\ B_3^\pm &= \frac{1}{4}(V_{\uparrow,\downarrow,\downarrow,\uparrow} \pm V_{\downarrow,\uparrow,\uparrow,\downarrow}), & B_4^\pm &= \frac{1}{4}(V_{\uparrow,\uparrow,\downarrow,\downarrow} \pm V_{\downarrow,\downarrow,\uparrow,\uparrow}), \\ B_5^\pm &= \frac{1}{4}(V_{\uparrow,\uparrow,\uparrow,\downarrow} \pm V_{\uparrow,\downarrow,\uparrow,\uparrow}), & B_6^\pm &= \frac{1}{4}(V_{\downarrow,\uparrow,\downarrow,\downarrow} \pm V_{\downarrow,\downarrow,\downarrow,\uparrow}), \\ B_7^\pm &= \frac{1}{4}(V_{\uparrow,\uparrow,\downarrow,\uparrow} \pm V_{\downarrow,\uparrow,\uparrow,\uparrow}), & B_8^\pm &= \frac{1}{4}(V_{\uparrow,\downarrow,\downarrow,\downarrow} \pm V_{\downarrow,\downarrow,\uparrow,\downarrow}). \end{aligned} \quad (8)$$

In Eqs. (8), we have omitted orbital guiding center indices for simplicity.

The many-electron state with pseudospin orientation \hat{m} is $|\Psi[\hat{m}]\rangle = \prod_{k=1}^{N_\phi} c_{\hat{m},k}^\dagger |0\rangle$, where $c_{\hat{m},k}^\dagger$ creates the single-particle state whose wave function is given in Eq. (5). We find that

$$\begin{aligned}
e_{\text{HF}}(\hat{m}) &\equiv \frac{\langle \Psi[\hat{m}] | H | \Psi[\hat{m}] \rangle}{N_\phi} \\
&= - \sum_{i=x,y,z} \left(b_i - \frac{1}{2} U_{1,i} - \frac{1}{2} U_{i,1} \right) m_i \\
&\quad + \frac{1}{2} \sum_{i,j=x,y,z} U_{i,j} m_i m_j, \tag{9}
\end{aligned}$$

where

$$U_{i,j} = \frac{1}{N_\phi} \sum_{k_1, k_2=1}^{N_\phi} (W_{i,j}^{k_1, k_2, k_1, k_2} - W_{i,j}^{k_2, k_1, k_1, k_2}) \tag{10}$$

has direct and exchange contributions. Equation (9) is the most general form for the HF energy of a pseudospin- $\frac{1}{2}$ QHF. The magnetic anisotropy of the particular QHF system is governed by the terms in Eq. (9) that are quadratic in the pseudospin magnetization m_i . The values of the coefficients $U_{i,j}$ depend on the nature of the crossing LLs and can result in isotropic, easy-plane, or easy-axis quantum Hall ferromagnetism.

IV. PSEUDOSPIN MATRIX ELEMENTS OF THE COULOMB INTERACTION

This section contains the derivation of explicit expressions for the anisotropy energy coefficients $U_{i,j}$, assuming the zero-width quantum-well model wave functions (1). Using the Fourier representation of the Coulomb interaction, we write the pseudospin matrix elements as

$$\begin{aligned}
V_{\sigma'_1, \sigma'_2, \sigma_1, \sigma_2}^{k'_1, k'_2, k_1, k_2} &= \frac{1}{A} \sum_q \delta_{q_y, k'_1 - k_1} \delta_{-q_y, k'_2 - k_2} \\
&\quad \times e^{iq_x(k'_1 + k_1)/2} e^{-iq_x(k'_2 + k_2)/2} v_{\sigma'_1, \sigma'_2, \sigma_1, \sigma_2}(\vec{q})
\end{aligned} \tag{11}$$

and hence

$$\begin{aligned}
&\frac{1}{N_\phi} \sum_{k_1, k_2=1}^{N_\phi} (V_{\sigma'_1, \sigma'_2, \sigma_1, \sigma_2}^{k_1, k_2, k_1, k_2} - V_{\sigma'_1, \sigma'_2, \sigma_1, \sigma_2}^{k_2, k_1, k_1, k_2}) \\
&= \frac{N_\phi}{A} v_{\sigma'_1, \sigma'_2, \sigma_1, \sigma_2}(0) - \frac{1}{A} \sum_q v_{\sigma'_1, \sigma'_2, \sigma_1, \sigma_2}(\vec{q}) \\
&= \int \frac{d^2 \vec{q}}{(2\pi)^2} e^{-q^2/2} [v_{\sigma'_1, \sigma'_2, \sigma_1, \sigma_2}(0) - v_{\sigma'_1, \sigma'_2, \sigma_1, \sigma_2}(\vec{q})].
\end{aligned} \tag{12}$$

Here l is the unit of length and $e^2/\epsilon l$ is the unit of energy. Note that $N_\phi/A = 1/2\pi$ in these units. The first factor in square brackets in this equation originates from the Hartree contribution to the energy while the second factor originates from the exchange contribution.

In these equations $v_{\sigma'_1, \sigma'_2, \sigma_1, \sigma_2}(\vec{q})$ is a pseudospin-dependent effective 2D interaction that, because of the separability of the in-plane and out-of-plane degree-of-freedom

terms in the single-electron Schrödinger equation, is the product of two factors: the subband factor

$$\begin{aligned}
v_{\sigma'_1, \sigma'_2, \sigma_1, \sigma_2}^{\Xi}(\vec{q}) &= \int_{-\infty}^{\infty} dz_1 \int_{-\infty}^{\infty} dz_2 e^{-q|z_1 - z_2|} \\
&\quad \times \lambda_{\xi(\sigma'_1)}(z_1) \lambda_{\xi(\sigma'_2)}(z_2) \lambda_{\xi(\sigma_1)}(z_1) \lambda_{\xi(\sigma_2)}(z_2)
\end{aligned} \tag{13}$$

and the in-plane term

$$\begin{aligned}
v_{\sigma'_1, \sigma'_2, \sigma_1, \sigma_2}^N(\vec{q}) &= e^{q^2/2} \int_{-\infty}^{\infty} dx_1 \phi_n(\sigma'_1, s(\sigma'_1), q_y/2(x_1)) \\
&\quad \times \phi_n(\sigma_1, s(\sigma_1), -q_y/2(x_1)) \\
&\quad \times \int_{-\infty}^{\infty} dx_2 \phi_n(\sigma'_2, s(\sigma'_2), -q_y/2(x_2)) \\
&\quad \times \phi_n(\sigma_2, s(\sigma_2), q_y/2(x_2)).
\end{aligned} \tag{14}$$

For a general sample geometry, the subband factor (13) has to be calculated numerically using the self-consistent LSDA wave functions. For our model bilayer system, however, we can obtain analytic expressions for $v_{\sigma'_1, \sigma'_2, \sigma_1, \sigma_2}^{\Xi}(\vec{q})$.

In the case of $\xi(\sigma) = \xi(-\sigma)$, Eqs. (1) and (13) give

$$v_{\sigma'_1, \sigma'_2, \sigma_1, \sigma_2}^{\Xi} = \frac{1}{2} [(1 + r_\Delta^2) + (1 - r_\Delta^2) e^{-dq}]. \tag{15}$$

In the second case, i.e., $\xi(\sigma) = -\xi(-\sigma)$,

$$v_{\sigma, \sigma, \sigma, \sigma}^{\Xi} = \frac{1}{2} [(1 + r_\Delta^2) + (1 - r_\Delta^2) e^{-dq}],$$

$$v_{\sigma, -\sigma, \sigma, -\sigma}^{\Xi} = \frac{1}{2} [(1 - r_\Delta^2) + (1 + r_\Delta^2) e^{-dq}],$$

(16)

$$v_{\sigma, -\sigma, -\sigma, \sigma}^{\Xi} = \frac{1}{2} (1 - r_\Delta^2) (1 - e^{-dq}),$$

$$v_{\sigma'_1, \sigma'_2, \sigma_1, \sigma_2}^{\Xi} = \eta \frac{r_\Delta}{2} (1 - r_\Delta^2)^{1/2} (1 - e^{-dq})$$

if $\eta \equiv \frac{1}{2} \sum_{i=1}^2 [\xi(\sigma'_i) + \xi(\sigma_i)] = \pm 1$.

For the in-plane factor in the effective interaction, it is necessary to distinguish several cases. If the pseudospin-up and pseudospin-down levels have the same real-spin index and the same orbit radius quantum number, i.e., $s(\sigma) = s(-\sigma)$ and $n(\sigma) = n(-\sigma) \equiv n$, the effective interaction is independent of the pseudospin indices and we obtain from Eqs. (2) and (14)

$$v_{\sigma'_1, \sigma'_2, \sigma_1, \sigma_2}^N = \frac{2\pi}{q} [L_n(q^2/2)]^2, \tag{17}$$

where $L_n(x)$ is the Laguerre polynomial. For identical spins but different orbit radius quantum numbers, i.e., $s(\sigma)$

$=s(-\sigma)$ and $n(\sigma) \neq n(-\sigma)$, we define $n_{<} \equiv \min[n(\sigma), n(-\sigma)]$ and $n_{>} \equiv \max[n(\sigma), n(-\sigma)]$. Then this factor in the effective interaction is

$$v_{\sigma,\sigma,\sigma,\sigma}^N = \frac{2\pi}{q} [L_{n(\sigma)}(q^2/2)]^2,$$

$$v_{\sigma,-\sigma,\sigma,-\sigma}^N = \frac{2\pi}{q} L_{n(\sigma)}(q^2/2) L_{n(-\sigma)}(q^2/2), \quad (18)$$

$$v_{\sigma,-\sigma,-\sigma,\sigma}^N = \frac{2\pi}{q} \frac{n_{>}!}{n_{<}!} \left(\frac{q^2}{2}\right)^{n_{>}-n_{<}} [L_{n_{<}}^{n_{>}-n_{<}}(q^2/2)]^2,$$

otherwise $v_{\sigma'_1, \sigma'_2, \sigma_1, \sigma_2}^N = 0$.

If the two pseudospin LLs have opposite real spins, then only scattering processes that conserve pseudospin (and therefore also real spin) at each vertex will contribute to the anisotropy energy. For $s(\sigma) = -s(-\sigma)$ and $n(\sigma) = n(-\sigma) \equiv n$, we obtain

$$v_{\sigma,\sigma,\sigma,\sigma}^N = v_{\sigma,-\sigma,\sigma,-\sigma}^N = \frac{2\pi}{q} [L_n(q^2/2)]^2, \quad (19)$$

otherwise $v_{\sigma'_1, \sigma'_2, \sigma_1, \sigma_2}^N = 0$.

Finally, if the pseudospin LLs have opposite real spins and different orbit radius quantum numbers, the in-plane factor in the effective interactions is

$$v_{\sigma,\sigma,\sigma,\sigma}^N = \frac{2\pi}{q} [L_{n(\sigma)}(q^2/2)]^2, \quad (20)$$

$$v_{\sigma,-\sigma,\sigma,-\sigma}^N = \frac{2\pi}{q} L_{n(\sigma)}(q^2/2) L_{n(-\sigma)}(q^2/2),$$

otherwise $v_{\sigma'_1, \sigma'_2, \sigma_1, \sigma_2}^N = 0$.

Equation (13) for the subband factor and explicit expressions (17)–(20) for the in-plane factor in the effective interaction, together with Eqs. (12), (10), (8), and Table I, provide a formal recipe to calculate the anisotropy coefficients $U_{i,j}$ for crossing LLs with any combination of quantum-well subband, orbit radius, and real-spin indices. In the following section, we use the explicit forms (16) and (15) for the subband factor to develop a pseudospin anisotropy classification scheme for our model bilayer system.

V. MAGNETIC ANISOTROPY

The nature of the anisotropy energy is of qualitative importance for two-dimensional ferromagnets, including QHFs. Systems with easy-axis anisotropy, i.e., discrete directions at which the energy of the ordered state is minimized, have long-range order at finite temperature and phase transitions in the Ising universality class. Systems with easy-plane anisotropy, i.e., a continuum of coplanar pseudospin magnetization orientations at which the energy of the ordered state is minimized, do not have long-range order but do have Kosterlitz-Thouless phase transitions at a finite temperature. In the isotropic case, all directions of pseudospin magnetiza-

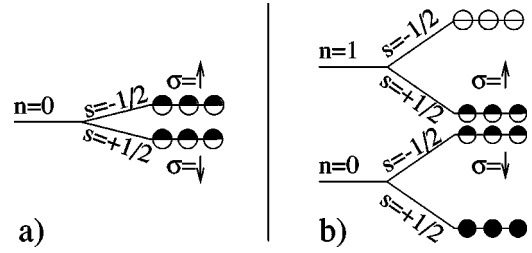


FIG. 2. Schematic LL diagrams for $\nu=1$ (a) and $\nu=2$ (b) single-subband QHFs. Index $\sigma=\uparrow, \downarrow$ labels the pseudospin LLs. The crossing LLs are indicated by half-solid dots, while inert filled LLs are indicated by solid dots and inert empty LLs by open dots.

tion have identical energy, only the ground state has long-range order, and there are no finite-temperature phase transitions. Nevertheless, magnetization correlations become extremely long at low temperatures. The objective of this work is to predict which class of QHF occurs for a particular pair of crossing LLs.

We start our analysis by considering pseudospin LLs that belong to the same subband, i.e., $\xi(\uparrow) = \xi(\downarrow)$. In this case, only LLs with opposite real spins can be aligned. Two examples of QHFs falling into this category—total filling factor $\nu=1$ with $n(\uparrow) = n(\downarrow) = 0$ and $\nu=2$ with $n(\uparrow) = 1$, $n(\downarrow) = 0$ —are illustrated in Fig. 2. The cases of $n(\uparrow) \neq n(\downarrow)$ are realized when the ratio of the spin splitting to LL separation is an integer. In GaAs, this ratio is only $\sim \frac{1}{60}$ at perpendicular fields but can be tuned by tilting the magnetic field away from the normal to the 2D layer. For typical widths, orbital effects of the in-plane field, not included here, become important at the tilt angles where the coincidences of interest are realized and have to be accounted for¹⁰ to obtain correct values of the pseudospin anisotropy energy coefficients (10). However, recent work on AlAs quantum wells¹⁷ and InSb quantum wells¹⁸ with large Zeeman couplings have made the situation that we study below, which assumes perpendicular magnetic field, accessible.

When opposite-spin LLs cross, Eqs. (19) and (20) imply that all interactions B_i^\pm with $i > 2$ in Eqs. (8) vanish. Then the only nonzero anisotropy term is

$$U_{z,z} = -\frac{1}{8} \int_0^\infty dq e^{-q^2/2} [L_{n(\uparrow)}(q^2/2) - L_{n(\downarrow)}(q^2/2)]^2 \times [(1+r_\Delta^2) + (1-r_\Delta^2)e^{-dq}]. \quad (21)$$

Note that the Hartree energy contribution to anisotropy always vanishes when the crossing LLs share the same subband wave function. If the two pseudospin levels also have the same orbit radius quantum number, then Eq. (21) gives $U_{z,z} = 0$ and the ferromagnetic state is *isotropic*. Physically, the result follows from the independence of the Coulomb interaction strength on real spin. An important example of these isotropic QHFs occurs when $n(\uparrow) = n(\downarrow) = 0$ and $r_\Delta = 1$, i.e., there is no tunneling between layers. This is the thoroughly studied single-layer $\nu=1$ QHF,²⁻⁴ for which the HF theory ground state happens to be exact. We remark that quantitative estimates based on the HF mean-field theory presented here require corrections to quantum fluctuation ef-

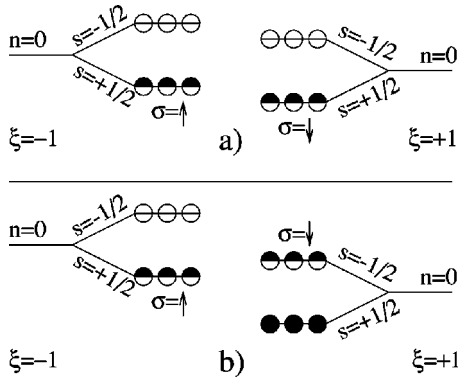


FIG. 3. Schematic LL diagrams for $\nu=1$ (a) and $\nu=2$ (b) bilayer QHFs. The pseudospin LLs have opposite subband indices and the same (a) or opposite (b) real spins.

fects in cases in which the ordered pseudospin moment direction is not a good quantum number. A detailed understanding of these corrections is one challenge for future experimental and theoretical work on QHFs.

For $n(\uparrow) \neq n(\downarrow)$, Eq. (21) implies that $U_{z,z} < 0$, making the z axis the easy pseudospin orientation axis. Again, at $r_\Delta = 1$ our model reduces to that of a single-layer 2D systems whose *easy-axis* anisotropy at even filling factors has been identified previously.¹⁰ In finite-thickness single quantum wells, a QHF with pseudospin LLs of the same subband but different real-spin and orbit radius indices is also *easy-axis*. The magnitude of the anisotropy will decrease with layer thickness, as can be seen by comparing $U_{z,z}$ in Eq. (21) calculated for $r_\Delta = 1$ and $r_\Delta = 0$. (Note that the single-subband unbiased double well with finite tunneling, i.e., $r_\Delta = 0$, models a single-layer system with an effective thickness d .)

We now turn to the crossing of LLs with different subband indices, for which the pseudospin anisotropy physics is richer. In Fig. 3, we show examples of $n(\uparrow) = n(\downarrow)$ bilayer QHFs for $\nu=1$ and $\nu=2$ based on the same real-spin and opposite real-spin LLs, respectively. Equations (10), (12), (16), (17), and Table I imply four nonzero anisotropy terms for $n(\uparrow) = n(\downarrow) \equiv n$ and $s(\uparrow) = s(\downarrow)$:

$$\begin{aligned} U_{z,z} &= ur_\Delta^2, \\ U_{x,x} &= u(1 - r_\Delta^2), \\ U_{x,z} &= U_{z,x} = ur_\Delta(1 - r_\Delta^2)^{1/2}, \end{aligned} \quad (22)$$

where

$$u = \frac{d}{2} - \frac{1}{2} \int_0^\infty dq e^{-q^2/2} [L_n(q^2/2)]^2 (1 - e^{-dq}).$$

The first term in the expression for energy u comes from the Hartree interaction. The second term represents the exchange contribution, which is always smaller than the Hartree energy in this case, i.e., $u > 0$. For zero tunneling between layers ($r_\Delta = 1$), the only nonzero anisotropy energy component, $U_{z,z} = u$, is positive, leading to the *easy-plane* anisotropy of the QHF. In the absence of symmetry-breaking fields [the

linear pseudospin magnetization terms in Eq. (9)], the variational energy (9) is minimized when the pseudospins condense into a state magnetized at an arbitrary orientation within the x - y plane. In this state, electronic charge is distributed equally between the layers (pseudospin angle $\theta = 0$) minimizing the electrostatic energy; spontaneous interlayer phase coherence,⁶ the physical counterpart of pseudospin order in this case, lowers the total energy of the system by strengthening interlayer exchange interactions.

For $r_\Delta^2 < 1$, Eqs. (22) imply the following quadratic terms in the HF total energy:

$$\sum_{i,j=x,y,z} U_{i,j} m_i m_j = u [r_\Delta m_z + (1 - r_\Delta^2)^{1/2} m_x]^2, \quad (23)$$

i.e., the easy plane is tilted from the x - y plane in the pseudospin space by angle $\alpha = \arctan[(1 - r_\Delta^2)^{1/2}/r_\Delta]$. The pseudospin basis states at different values of r_Δ are related, however, by a unitary transformation, which corresponds precisely to a rotation about the y axis by angle $-\alpha$, as seen from Eq. (1). The easy plane where the above anisotropy energy is constant is, for any value of r_Δ , the plane of equal charge per layer.

When pseudospin-up and pseudospin-down states differ by more than their subband indices, by their spin indices for example, the two pseudospin basis states at different r_Δ are not related by a unitary transformation. In this case, the magnetic anisotropy does depend on r_Δ . For example, consider the case $\xi(\uparrow) = -\xi(\downarrow)$, $n(\uparrow) = n(\downarrow)$, and $s(\uparrow) = -s(\downarrow)$. For opposite real-spin LLs, all anisotropy terms that include pseudospin nonconserving scattering processes drop out. The only nonzero energy term, $U_{z,z}$, has the same value as in Eq. (22). Hence, the QHF is *isotropic* in the unbiased ($r_\Delta = 0$) bilayer system while applying external bias ($r_\Delta > 0$) leads to *easy-plane* anisotropy in pseudospin space.

At this point let us make an experimentally important comment on the bilayer systems realized in wide single quantum wells.^{2,9,19} The difference between this sample geometry and the double quantum well with narrow (in our model infinitely narrow) layers is in the nature of the barrier responsible for the bilayer character of the electronic system. In wide quantum wells the barrier is soft,¹⁹ originating from Coulomb interactions among electrons in the well. Then the tunneling probability between layers is strongly dependent on the electron density and quantum-well subband populations. This tunability makes wide single quantum wells an experimentally attractive alternative to double wells in studies of bilayer quantum Hall phenomena. The softness of the barrier can, however, lead to qualitatively important consequences for the ordered many-particle states. Translated into the pseudospin language, Δ_t cannot be treated as an external one-body field acting on the pseudospin particles but, in general, will depend¹¹ on the pseudospin orientation in the ordered ground state. For the pseudospin LLs discussed in the preceding paragraph [$\xi(\uparrow) = -\xi(\downarrow)$, $n(\uparrow) = n(\downarrow)$, and $s(\uparrow) = -s(\downarrow)$] and for $r_\Delta = 0$, this effect can lead to an anisotropic QHF. LSDA calculations indicate that at low electron densities, the anisotropy will be *easy-plane* while *easy-axis* anisotropy is more likely to develop at high densities.¹¹ We

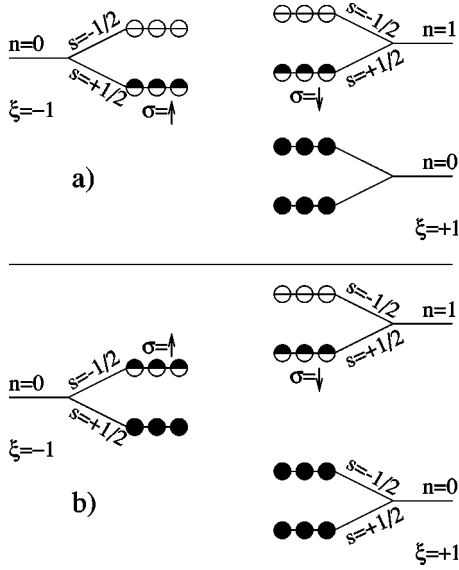


FIG. 4. Schematic LL diagrams for $\nu=3$ (a) and $\nu=4$ (b) bilayer QHFs. The pseudospin LLs have opposite subband indices, different orbit radius quantum numbers, and the same (a) or opposite (b) real spins.

make this remark to point out that not all results obtained for the double-quantum-well model are directly applicable to bilayers in wide single wells. In many cases, the theoretical description of QHFs in wide single wells requires modifications of the idealized bilayer model to account for mixing of higher electrical subbands. The self-consistent LSDA for the growth direction single-particle orbitals is a particularly convenient, if somewhat *ad hoc*, method that allows any sample geometry to be studied while retaining the basic structure of the many-body HF formalism for QHFs.

In the remaining part of this section, we consider pseudospin LLs with opposite subband indices *and* different orbit radius quantum numbers. At total filling factor $\nu=3$, for example, the pseudospin LLs will have the same real spin, while at $\nu=4$ opposite-spin LLs can be aligned, as shown in Fig. 4. A common feature of the QHFs discussed below is the transition from a state with easy-axis anisotropy to a state with easy-plane anisotropy as r_Δ and the layer separation d are varied. For $s(\uparrow)=s(\downarrow)$, Eqs. (10), (12), (16), (18), and Table I give three nonzero anisotropy energies,

$$\begin{aligned}
 U_{z,z} &= \frac{r_\Delta^2 d}{2} - \frac{1}{8} \int_0^\infty dq e^{-q^2/2} \{ [L_{n(\uparrow)}(q^2/2) - L_{n(\downarrow)}(q^2/2)]^2 \\
 &\quad \times (1 + e^{-dq}) + r_\Delta^2 [L_{n(\uparrow)}(q^2/2) + L_{n(\downarrow)}(q^2/2)]^2 \\
 &\quad \times (1 - e^{-dq}) g \}, \\
 U_{x,x} = U_{y,y} &= -\frac{1}{4} \int_0^\infty dq e^{-q^2/2} \frac{n_{<}}{n_{>}} \left(\frac{q^2}{2} \right)^{n_{>} - n_{<}} \\
 &\quad \times [L_{n_{<}}^{n_{>} - n_{<}}(q^2/2)]^2 (1 - r_\Delta^2) (1 - e^{-dq}), \quad (24)
 \end{aligned}$$

where

$$n_{<} \equiv \min[n(\uparrow), n(\downarrow)], \quad n_{>} \equiv \max[n(\uparrow), n(\downarrow)].$$

The HF total energy contributions that are quadratic in the pseudospin magnetization components can be grouped as

$$\sum_{i,j=x,y,z} U_{i,j} m_i m_j = (U_{z,z} - U_{x,x}) m_z^2 + U_{x,x}. \quad (25)$$

(Recall that \hat{m} is a unit vector, i.e. $m_x^2 + m_y^2 = 1 - m_z^2$.) From Eq. (25), we obtain that for $U_{z,z} - U_{x,x} < 0$ the QHF has *easy-axis* anisotropy while for $U_{z,z} - U_{x,x} > 0$ the system is an *easy-plane* ferromagnet. At the critical layer separation $d = d^*$, obtained from the condition $U_{z,z} = U_{x,x}$, the magnetic anisotropy vanishes and a fine-tuned isotropy is achieved. It follows from Eqs. (24) that d^* is finite for all values of r_Δ .

For pseudospin LLs with $s(\uparrow) = -s(\downarrow)$, the anisotropy energy components $U_{x,x}$ and $U_{y,y}$ vanish and the critical layer separation d^* corresponds to $U_{z,z} = 0$, where $U_{z,z}$ is given by the same expression as in the $s(\uparrow) = s(\downarrow)$ case [see Eq. (24)]. Since $U_{z,z} < 0$ at $r_\Delta = 0$, the critical separation d^* diverges in the absence of external bias, i.e., easy-axis pseudospin anisotropy does not exist for any layer separation. For $r_\Delta > 0$, the transition between easy-plane and easy-axis anisotropy occurs at finite d as for the $s(\uparrow) = s(\downarrow)$ pseudospin LLs.

In Figs. 5(a) and 5(b), we show the magnetic anisotropy phase diagrams in the d - r_Δ plane calculated for $\nu=3$ and $\nu=4$ QHFs (see Fig. 4). Since the layer separation is in units of magnetic length, these figures imply that transition between easy-axis and easy-plane anisotropies at a given filling factor can be induced in one physical sample by changing the density of the 2D electron system. High electron densities would correspond to the easy-plane region, and low densities to the easy-axis region. Note that these numerical results confirm the general remark made above, since the critical layer separation diverges as $r_\Delta \rightarrow 0$ for $\nu=4$ while it remains finite for $\nu=3$.

VI. SYMMETRY-BREAKING FIELDS

The pseudospin orientation in a QHF ground state is determined by minimizing the variational total energy (9). In the absence of energy terms that are linear in pseudospin magnetization components, the HF ordered states spontaneously break continuous SU(2) or U(1) symmetry⁶ in the case of isotropic or easy-plane QHFs, respectively, and the discrete symmetry between pseudospin-up and pseudospin-down orientations in the case of easy-axis QHFs. In this section, we take into account external and internal potentials that contribute to the linear terms in the HF total energy and we comment on the pseudospin reversal that can be triggered by adjusting these symmetry-breaking fields. We focus on a case that we feel is particularly appropriate for experimental study by considering the ordered $\nu=3$ quantum Hall state. Similar considerations would apply for all classes of QHFs discussed in this paper.

The pseudospin LLs in the bilayer $\nu=3$ QHF (see Fig. 4) have opposite subband indices and orbit radius quantum

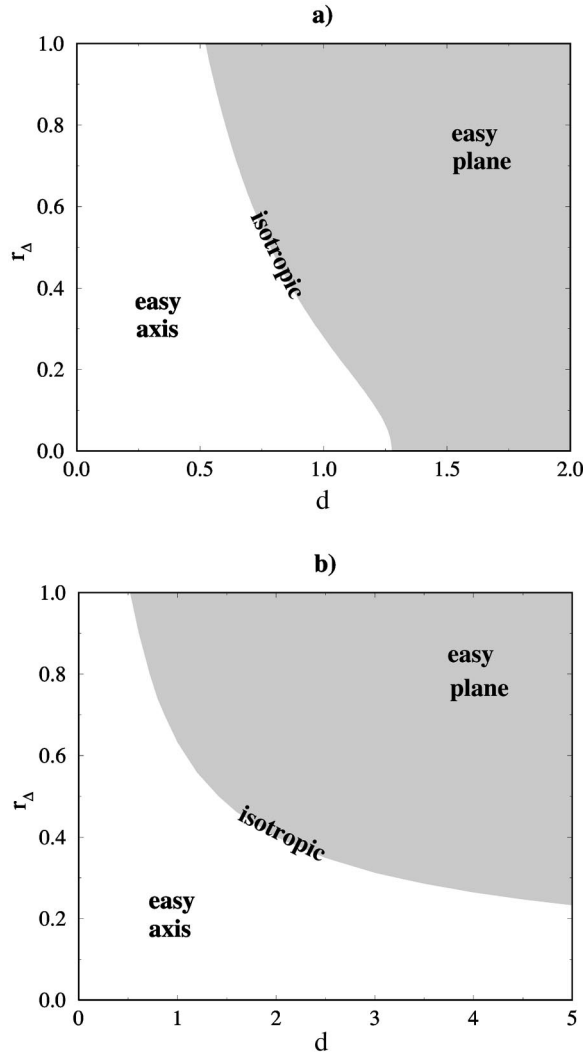


FIG. 5. Magnetic anisotropy phase diagrams for bilayer $\nu=3$ (a) and $\nu=4$ (b) QHFs from Fig. 4. In the white region the anisotropy is easy-axis, in the gray region the QHF has easy-plane anisotropy. At the phase boundary the ferromagnetic state is isotropic.

numbers $n=0$ and $n=1$, respectively. We call the $[\xi=-1, n=0, s=+\frac{1}{2}]$ LL the pseudospin-up state and the $[\xi=1, n=1, s=+\frac{1}{2}]$ LL the pseudospin-down state. With this definition, the one-body potentials in Eq. (9) can be written as

$$\begin{aligned}
 b_z &= -\frac{1}{2}[(\Delta_V^2 + \Delta_I^2)^{1/2} - \hbar\omega_c + I_F - I_{H,z}], \\
 b_x &= \frac{1}{2}I_{H,x}, \\
 b_y &= 0.
 \end{aligned} \tag{26}$$

The effective field I_F is the difference between pseudospin-up and pseudospin-down particle exchange energy with electrons in the fully occupied $[\xi=1, n=0, s=+\frac{1}{2}]$ LL, i.e.,

$$\begin{aligned}
 I_F &= \frac{1}{2} \int_0^\infty dq e^{-q^2/2} \left\{ \frac{q^2}{2} [1 + r_\Delta^2 + (1 - r_\Delta^2)e^{-dq}] \right. \\
 &\quad \left. - (1 - r_\Delta^2)(1 - e^{-dq}) \right\}. \tag{27}
 \end{aligned}$$

For $r_\Delta > 0$, electrons in the $[\xi=1, n=0, s=\pm\frac{1}{2}]$ LLs produce also an electrostatic field, represented by $I_{H,z}$ and $I_{H,x}$ in Eqs. (26), which screens the external bias potential. Since this effective field favors occupation of a particular layer rather than a particular pseudospin state, it couples to z and x components of the pseudospin operator. The energy imbalance between the two layers produced by \vec{I}_H is $2dr_\Delta$, which, together with Eq. (1), gives

$$I_{H,z} = 2dr_\Delta^2,$$

$$I_{H,x} = 2dr_\Delta(1 - r_\Delta^2)^{1/2}. \tag{28}$$

In the expression for the HF total energy (9), we included explicitly the contribution to the symmetry-breaking fields that results from Coulomb interactions between electrons in the pseudospin LLs. For the $\nu=3$ QHF we are considering here, only $U_{1,z}$ and $U_{z,1}$ energies are nonzero:

$$\begin{aligned}
 U_{1,z} = U_{z,1} &= -\frac{1}{8} \int_0^\infty dq e^{-q^2/2} [1 + r_\Delta^2 + (1 - r_\Delta^2)e^{-dq}] \\
 &\quad \times (q^2 - q^4/4). \tag{29}
 \end{aligned}$$

In the bilayer system with no tunneling ($r_\Delta=1$), $I_{H,x}=0$ and the total symmetry breaking field, $b^* \equiv b_z - U_{1,z}$, is oriented along the z pseudospin direction and is given by

$$b^* = -\frac{1}{2}[(\Delta_V^2 + \Delta_I^2)^{1/2} - \hbar\omega_c + \sqrt{\pi/2}/2 - 2d - \sqrt{\pi/2}/8]. \tag{30}$$

In Figs. 6(a)–6(c), we plot the pseudospin evolution with effective field b^* for the three anisotropy regimes of a $\nu=3$ QHF with $r_\Delta=1$. At the phase boundary between easy-axis and easy-plane anisotropies, the $\nu=3$ QHF is isotropic and the pseudospin reverses abruptly at $b^*=0$ [see Fig. 6(a)]. In the easy-plane anisotropy regime, ($U_{z,z} - U_{x,x} > 0$), the pseudospin evolves continuously with b^* as illustrated in Fig. 6(b), reaching alignment with b^* at $|b^*| \geq U_{z,z} - U_{x,x}$. For the easy-axis anisotropy case ($U_{z,z} - U_{x,x} < 0$), the HF energy has two local minima at $m_z = \pm 1$ when $|b^*| < |U_{z,z} - U_{x,x}|$. The pseudospin-up and pseudospin-down polarized states are separated by an energy barrier that results in the hysteretic pseudospin-reversal behavior shown in Fig. 6(c).

In bilayer systems with nonzero tunneling, pseudospin reversal follows a more complicated pattern in which the competition between x and z components of the symmetry-breaking field plays an important role. In general, the pseudospin will rotate in the x - z plane, i.e., $m_x = \sqrt{1 - m_z^2}$. Since the derivative of the HF energy with respect to m_z

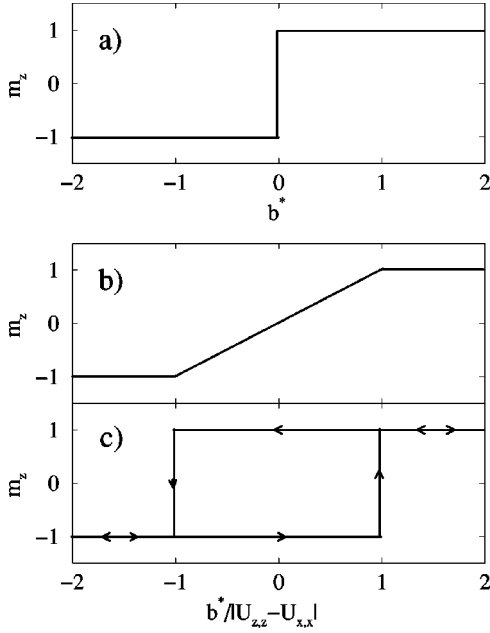


FIG. 6. Pseudospin orientation as a function of the effective field b^* for the isotropic QHF and as a function of b^* relative to the anisotropy energy $|U_{z,z} - U_{x,x}|$ for the easy-plane (b), and easy-axis (c) QHFs at $\nu=3$.

diverges at $m_z = \pm 1$ due to the $I_{H,x}$ term, the pseudospin will never align completely with the z axis when $r_\Delta < 1$.

VII. SUMMARY

In the strong magnetic-field limit, the physics of high mobility two-dimensional electron systems is usually dominated by electron-electron interactions except at integer filling factors, where the single-particle physics responsible for the gap between Landau levels assumes the dominant role. When external parameters are adjusted so that two or more Landau levels simultaneously approach the chemical potential, the integer filling factor case is less exceptional, interaction effects are always strong, and uniform density broken-symmetry ground states analogous to those in conventional ferromagnets are common. In this paper, we have discussed how the nature of these states depends on the character of the nearly degenerate Landau levels. Our attention is restricted to the case where only two Landau levels are close to the chemical potential and we distinguish these crossing Landau levels by introducing a pseudospin degree of freedom.

Using Hartree-Fock variational wave functions, we are able to derive an explicit expression for the dependence of ground-state energy on pseudospin orientation for crossing LLs with any combination of quantum-well subband, orbit radius, and real-spin degree-of-freedom quantum numbers. As in conventional magnetic systems, qualitative differences exist between the physical properties of isotropic (Heisenberg) systems with no dependence of energy on pseudospin orientation, easy-axis (Ising) systems with discrete preferred pseudospin orientations, and (XY) easy-plane systems for which the minimum is achieved simultaneously for a plane

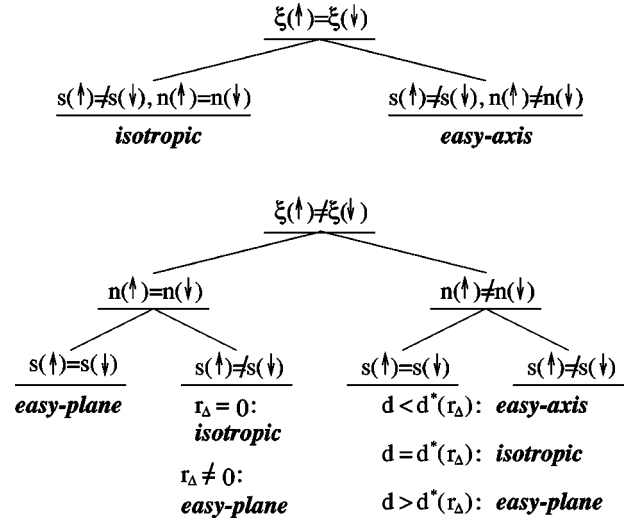


FIG. 7. Magnetic anisotropy of QHFs with pseudospin LL subband indices $\xi(\sigma)$, orbit radius quantum numbers $n(\sigma)$, and real spins $s(\sigma)$.

of orientations. Our mean-field results predict which class of pseudospin quantum Hall ferromagnet occurs in different circumstances. We focus on a model commonly used for bilayer quantum Hall systems in which the finite width of both quantum wells is neglected. The external parameters of the model are the Zeeman coupling strength, the bias potential between the wells Δ_V , and the single-particle splitting due to interlayer tunneling Δ_I . In the limit $\Delta_I=0$, this model applies to a single quantum well when the crossing Landau levels have the same subband wave function, i.e., are in the same quantum well. Classification predictions for this model as a function of layer separation d and the ratio $r_\Delta = \Delta_V / (\Delta_V^2 + \Delta_I^2)^{1/2}$ are summarized in Fig. 7.

For the single-quantum-well case, we find isotropic behavior when the orbit radius quantum numbers of the crossing Landau levels are identical, and easy-axis behavior otherwise. In general, when the crossing Landau levels have identical subband wave functions, the nature of the pseudospin anisotropy does not depend on the parameters d and r_Δ . For different subband wave functions, the pseudospin anisotropy can vary in the d - r_Δ plane. Particularly intriguing is the case of crossing LLs with different subband and orbit radius quantum numbers where, at a given filling factor, the system can undergo a quantum phase transition from an easy-axis to easy-plane QHF. At the phase boundary, the pseudospin anisotropy vanishes and a fine-tuned isotropy is achieved. The critical values of d and r_Δ are experimentally accessible and may be accompanied by observable changes in pseudospin reversal properties as external parameters are varied.

ACKNOWLEDGMENTS

This work was supported by the National Science Foundation under Grants No. DMR-9623511, No. DMR-9714055, and No. DGE-9902579 and by the Grant Agency of the Czech Republic under Grant No. 202/98/0085.

- ¹A. H. MacDonald, in *Proceedings of the 1994 Les Houches Summer School on Mesoscopic Quantum Physics*, edited by E. Akkermans *et al.* (Elsevier Science, Amsterdam, 1995), pp. 659–720.
- ²For a review on QHFs at $\nu=1$, see the experimental chapter by J. P. Eisenstein and the theoretical chapter by S. M. Girvin and A. H. MacDonald, in *Perspectives on Quantum Hall Effects* (Wiley, New York, 1997).
- ³C. Kallin and B. I. Halperin, Phys. Rev. B **30**, 5655 (1984); D. H. Lee and C. L. Kane, Phys. Rev. Lett. **64**, 1313 (1990); S. L. Sondhi, A. Karlhede, S. A. Kivelson, and E. H. Rezayi, Phys. Rev. B **47**, 16 419 (1993); A. H. MacDonald, H. A. Fertig, and L. Brey, Phys. Rev. Lett. **76**, 2153 (1996).
- ⁴S. E. Barrett, G. Dabbagh, L. N. Pfeiffer, and K. W. West, Phys. Rev. Lett. **74**, 5112 (1995); R. Tycko, S. E. Barrett, G. Dabbagh, L. N. Pfeiffer, and K. W. West, Science **268**, 1460 (1995); A. Smeller, J. P. Eisenstein, L. N. Pfeiffer, and K. W. West, Phys. Rev. Lett. **75**, 4290 (1995); D. K. Maude, M. Potemski, J. C. Portal, M. Henini, L. Eaves, G. Hill, and M. A. Pate, *ibid.* **77**, 4604 (1996); E. H. Aifer, B. B. Goldberg, and D. A. Broido, *ibid.* **76**, 680 (1996); V. Bayot, E. Grivei, J. M. Beuken, S. Melinte, and M. Shayegan, *ibid.* **76**, 4584 (1996); **79**, 1718 (1997).
- ⁵A. H. MacDonald, P. M. Platzman, and G. S. Boebinger, Phys. Rev. Lett. **65**, 775 (1990).
- ⁶T. Chakraborty and Pietiläinen, Phys. Rev. Lett. **59**, 2784 (1987); X. G. Wen and A. Zee, Phys. Rev. B **47**, 2265 (1993); Z. F. Ezawa and A. Iwazaki, Int. J. Mod. Phys. B **19**, 3205 (1992); L. Brey, Phys. Rev. Lett. **65**, 903 (1990); H. A. Fertig, Phys. Rev. B **40**, 1087 (1989); O. Narikiyo and D. Yoshioka, J. Phys. Soc. Jpn. **62**, 1612 (1993); R. Côté, L. Brey, and A. H. MacDonald, Phys. Rev. B **46**, 10 239 (1992); X. M. Chen and J. J. Quinn, *ibid.* **45**, 11 054 (1992); K. Moon *et al.*, *ibid.* **51**, 5138 (1995); K. Yang *et al.*, *ibid.* **54**, 11 644 (1996).
- ⁷I. B. Spielman, J. P. Eisenstein, L. N. Pfeiffer, and K. W. West, Phys. Rev. Lett. **84**, 5808 (2000).
- ⁸S. Q. Murphy, J. P. Eisenstein, G. S. Boebinger, L. N. Pfeiffer, and K. W. West, Phys. Rev. Lett. **72**, 728 (1994).
- ⁹T. S. Lay, Y. W. Suen, H. C. Manoharan, X. Ying, M. Santos, and M. Shayegan, Phys. Rev. Lett. **50**, 17 725 (1994); M. Abolfath, R. Golestanian, and T. Jungwirth, Phys. Rev. B **61**, 4762 (2000).
- ¹⁰T. Jungwirth, S. P. Shukla, L. Smrčka, M. Shayegan, and A. H. MacDonald, Phys. Rev. Lett. **81**, 2328 (1998).
- ¹¹V. Piazza, V. Pellegrini, F. Beltram, W. Wescheider, T. Jungwirth, and A. H. MacDonald, Nature (London) **402**, 638 (1999).
- ¹²G. F. Giuliani and J. J. Quinn, Phys. Rev. B **31**, 6228 (1985).
- ¹³Recently observed hysteresis at $\nu=\frac{2}{5}$ and $\frac{4}{9}$, corresponding to composite fermion filling factors $\nu=2$ and 4, has also been interpreted within the easy-axis QHF framework: H. Cho, J. B. Young, W. Kang, K. L. Campman, A. C. Gossard, M. Bichler, and W. Wescheider, Phys. Rev. Lett. **81**, 2522 (1998).
- ¹⁴L. Zheng, R. J. Radtke, and S. Das Sarma, Phys. Rev. Lett. **78**, 2453 (1997); S. Das Sarma, S. Sachdev, and L. Zheng, *ibid.* **79**, 917 (1997); Phys. Rev. B **58**, 4672 (1998); L. Brey, E. Demler, and S. Das Sarma, Phys. Rev. Lett. **83**, 168 (1999); B. Paredes, C. Tejedor, L. Brey, and L. Martín-Moreno, *ibid.* **83**, 2250 (1999).
- ¹⁵V. Pellegrini, A. Pinczuk, B. S. Dennis, A. S. Plaut, L. N. Pfeiffer, and K. W. West, Phys. Rev. Lett. **78**, 310 (1997); Science **281**, 799 (1998); A. Sawada, A. F. Ezawa, H. Ohno, Y. Horikoshi, Y. Ohno, S. Kishimoto, and F. Matsukura, Phys. Rev. Lett. **80**, 4534 (1998).
- ¹⁶G. Bastard, *Wave Mechanics Applied to Semiconductor Heterostructures* (Les Éditions de Physique, Paris, 1990).
- ¹⁷S. J. Papadakis, E. P. De Poortere, and M. Shayegan, Phys. Rev. B **59**, R12 743 (1999).
- ¹⁸K. J. Goldammer, S. J. Chung, W. K. Liu, M. B. Santos, J. L. Hicks, S. Raymond, and S. Q. Murphy, J. Cryst. Growth **202**, 753 (1999).
- ¹⁹Y. W. Suen, J. Jo, M. B. Santos, L. W. Engel, S. W. Hwang, and M. Shayegan, Phys. Rev. B **44**, 5947 (1991); T. S. Lay, T. Jungwirth, L. Smrčka, and M. Shayegan, *ibid.* **56**, R7092 (1997).